LAWRENCE
LIVERMORE
NATIONAL
LABORATORY

LLNL-TR-662536

Report on Sabbatical activities- Dr. Ronnie Shepherd-05/25/2014 to 08/21/2014

R. Shepherd

October 13, 2014

This work performed under the auspices of the U.S. Department of Energy by Lawrence Livermore National Laboratory under Contract DE-AC52-07NA27344.

Report on Sabbatical activities- Dr. Ronnie Shepherd-05/25/2014 to 08/21/2014

Introduction

The sabbatical performed by Dr. Ronnie Shepherd from 05/25/2014 to 08/21/2014 had two central goals: 1) write three proposals for future collaborative experiments at Ecole Polytechnique (and possibly LLNL) 2) if laser time was granted (based on the proposal), perform a preliminary experiment in preparation for the campaign of laser time based on proposal submission.

A team of scientists was formed for the collaboration. In addition to myself, the team consisted on Dr. Bérénice Loupias , Dr. Patrick Renaudin, Dr. Charles Reverdin from Commissariat à l'énergie atomique et aux energies alternatives (CEA), Dr. Patrick Audebert, Sophie Baton, Dr. Ludovic Lecherbourg, Dr. Serres Fabien, from Laboratoire d'Utilization des Lasers Intenses (LULI/Ecole Polytechnique) and students Vincent Dervieux and Alexandre Do (Ecole Polytechnique).

Scientific Proposals

Three concepts were explored during the proposal writing phase, namely 1) experiments to study hot electron heating in short pulse laser heated solids, 2) production of high pressure, high density matter using short pulse laser heated buried layers and 3) utilization of high repetition rate, short pulse laser generated neutrons. All three areas of research would provide important scientific information to the field of short pulse laser heated matter.

Study of damping rate of non-thermal, short pulse laser generated electrons

The interest in the time history of short pulse laser generated electrons is motivated by the use of this platform to generate (nearly) gradient free, high temperature, high-density plasmas to study opacities. Although the platform has shown promise of fulfilling this goal, serious questions remain about the heating process due to the damping of the hot electrons. To study of the time-history of hot electrons (generated when a high intensity, short pulse laser interacts with matter), an experiment utilizing K_α emission was proposed. The laser generated, non-thermal electrons collide with bound electrons (N=1), producing inner-shell holes, resulting in the prompt cascading of upper-state electrons to fill the holes. As the upper-state electrons fill the holes, K_α emission occurs. After the hole is created (by the hot electron), the K_α photon is rapidly emitted (due to the large Einstein coefficient for spontaneous emission). As a result, the K_α emission can be used as a sort of prompt "scintillator". If the ion is chosen such that the population of electrons in the tail generates few inner shell holes, then the dominant source of hole-states will result from non-thermal electron collisions or,

$$N_{n-1} \propto N_0 \bullet (\sigma_{BEB}(E) \bullet \rho_A \bullet L) \bullet N_h,$$

where, N_{n-1} is the number of ions in the target with inner-shell holes, N_0 is the number of ions/atom without inner-shell electrons removed, $\sigma_{BEB}(E)$ is the energy dependent inner-shell ionization cross-section, ρ_A is the target density, L is the propagation distance the hot electrons travel through the target, and N_h is the number of hot electrons traveling through the target. The intensity of the K_α is,

$$I_{K_\alpha} \propto (4\pi)^{-1}(hc/\lambda_0)A_{ki}N_{n-1}L,$$

where, h *and* c are Planck's constant and the speed of light, respectively, λ_0 is the wavelength of the K_α, and A_{ki} is the spontaneous emission Einstein coefficient for the K_α. Thus, from the observed x-ray signal we can infer the number electrons that produce K_α above the detection threshold. The signal measured by the streak camera is can be used to determine the time at which the bulk of the hot electron population's energy drops below the binding energy for the inner shell electron. An illustration of the experimental configuration is shown in figure 1.

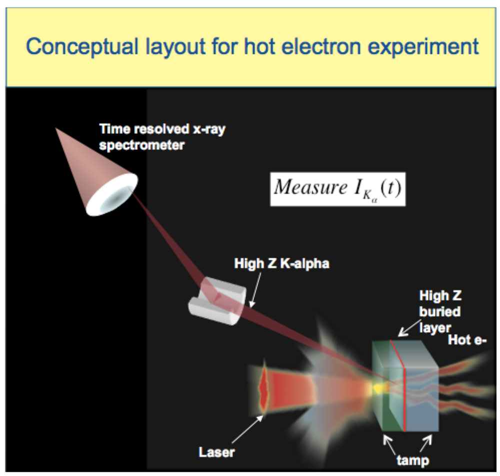

Figure 1: Experimental configuration for measuring time-resolved relaxation of non-thermal electrons

This idea was proposed in 2004[1] and was shown to be successful[2]. However, limited data was collected and a more detailed study of the evolution of the hot electron energy distribution is desired to thoroughly understand the hot electron energy transfer to the thermal electrons in the solid. In the previous application, the time-dependent emission of the Ti-K_α was used to determine the time required for non-thermal electron's energy to go below 4.5 keV (~11 ps). This experiment was performed using a single K_α emitter (Ti). The result provides one energy/time point in the evolution process. A more detailed determination of the temporal evolution would involve several energy/time points to map the energy transfer time. This measurement requires using multiple K_α emitters (ideally in the same shot).

In adding K_α emitters to the target, several issues must be taken into consideration. Since the initial temperature of the non-thermal electrons is very high ($\gtrsim$ 300 keV), an energy point much greater than 4.5 keV would be ideal. However, as the photon energy increases, the photocathode response on the streak camera decreases. The sensitivity above 10 keV for typical photocathodes (e.g., CsI) becomes extremely poor[3]. Taking these issues into consideration, Cu (K_α~8 keV) and Zr (K_α~16 keV) have been chosen. Although these energy points are significantly less than the initial non-thermal electron energy, the energy spacing is a factor two and this should provide some idea of the energy exchange trend.

Additionally, the time-dependent electron thermal temperature will be measured using an aluminum K-shell tracer. The K-shell tracer will provide a monitor of the peak thermal temperature achieved in the plasma. A comparison between the heating time of the thermal electrons and the damping time of the hot electron bath will provide insight into the energy transfer/plasma heating process.

The experiment requires one (possibly two) ultrafast x-ray streak cameras. The LLNL ultrafast TREX streak camera has been provided as a primary diagnostic. If possible, it will measure both Al K-shell emission and Ti, Cr, Zr K_α emission.

Production of short lived, isomeric low-lying nuclear levels using high intensity, short pulse laser-solid interactions.

Nuclear excitation is primarily calculated for neutral atoms. Because of the energy difference between excited nuclear states and atomic transitions, this approach is adequate for most nuclear transitions. However, for low-lying nuclear transitions, atomic excitation or plasma free electrons can result in populating nuclear excited states[4]. In fact, since all high Z nuclear transitions in stellar interiors occur in plasmas, these transitions must participate in the energy balance of stellar interiors.

In addition to inelastic scattering collision with high Z nuclei in plasmas, plasmas can create nuclear excitation by two methods; 1) nuclear excitation by electron capture (NEEC) and 2) nuclear excitation by electron transition (NEET). NEEC can occur when a free electron is captured into a bound state and the virtual photon emitted is absorbed by the nucleus. Alternatively, a bound electron may be excited by either electron collision or photo-excitation and upon de-excitation the resulting photon is absorbed by the nucleus (NEET). Although both methods of nuclear excitation is possible in a plasma, the later is more difficult due to the narrower atomic/nuclear overlap. Our work will focus on successfully measuring NEEC in well characterized plasmas.

Observing the low-lying nuclear transitions is challenging due to atomic emission in the same spectral range. However, the low-lying nuclear transitions tend to be long (> 1 ns) while the inherent atomic transition rates tend to fast (≤ 1 ps) but will continue as long as the plasma conditions are sustained. If the excitation source is rapidly removed for both atomic and nuclear levels of similar energies, the nuclear levels will tend to naturally live longer. We will utilize this fact by using a short pulse laser to heat a high Z target to provide a sufficiently high temperature environment to generate NEEC. Additionally, the targets will be designed to minimize expansion and maintain a high density. Under these conditions, radiative cooling is rapid (as short as a few ps[5]), the temporal emission from atomic transitions will be short, potentially leaving only the emission from the low-lying nuclear transitions. This would be the first observation of NEEC.

This project idea was unsuccessfully submitted several years ago as an LDRD. During the sabbatical time, this concept was revisited and evaluated. Other approaches were considered (including using protons). In the end, the original idea was found to be the most practical approach to studying NEEC/NEET processes. A review (and update) of this plan is submitted here.

Project Plan

The project will use a short pulse laser to heat a solid target to a temperature of $T_e \geq 500$ eV. As mentioned in the introduction, critical to observing NEEC is controlling the competing atomic emission. Ideally, theories of plasma-excited nuclear states would be tested quantitatively for two parameters: 1) the plasma conditions (ρ, T_e) when the nuclear excited state is generated and 2) the temporal lifetime of the excited state. In order to quantitatively test NEEC theories, a platform that allows for uniform plasma conditions is desirable. Since the temporal differences in the atomic and nuclear emission will be used to isolate the NEEC event, the energy sensitivity of time-resolved detectors must be considered as well in designing the experimental platform. At sufficiently high energies (> 10 keV, high-resolution (≤ 30 ps) x-ray detectors lose sensitivity. Thus it is preferable that the candidate nuclei have an excited state ≤ 10 keV. Also, because the measurement will require some minimal number of photons per picosecond, the nuclear emission should not occur over a period that is too long or the emission rate may be inadequate to detect.

Given these requirements, the targets will be designed such that a high Z layer will be sandwiched between two low Z layers (buried layer). When heated, the high Z layer will be confined until the inertial mass of the low Z layer has decompressed. This will help maintain uniform plasma conditions (ρ, T_e) while the nuclear states are being excited. The high Z layer will be doped with a tracer material to help characterize the plasma density and temperature. The dopant will be an element that emits atomic K-shell emission outside of the emission range of the high-Z layer at the expected temporal range. The time history of the tracer K-shell emission will be used as a plasma diagnostic.

We have looked at potential candidates for the excited nuclear state and reduced the list to a few choices. The top candidate is ^{169}Tm. The excited nuclear transition energy is 8.4 keV and has a half-life of 4.1 ns. The energy is within the sensitivity range of the time-resolved x-ray detectors and the half-life is sufficiently short that our time-resolved detectors should capture the majority of the emission from the emitting nuclei. An illustration of the atomic capture process leading to excited nuclear transition in thulium is shown in figure 1.

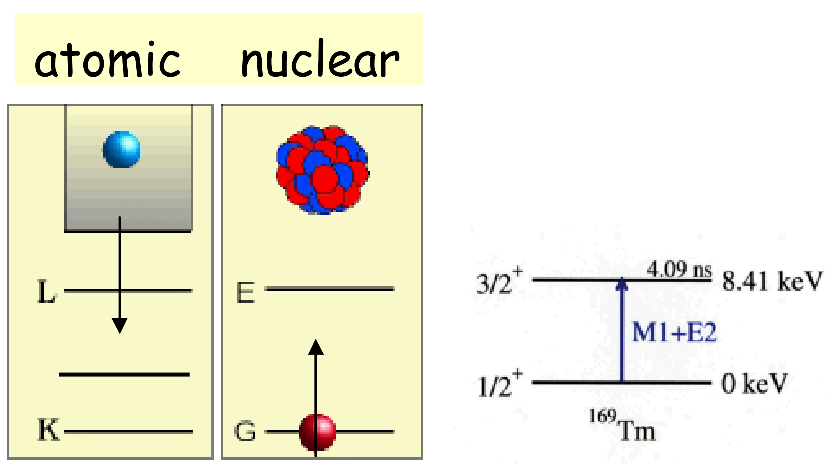

Figure 1: Illustration of the NEEC process in ^{169}Tm (atomic capture leading to an excited nuclear state).

Current Buried Layer Research

The platform for the experiments will be short pulse laser heated buried layers. In recent years, short pulse laser heated buried layers have successfully generated high temperature, high density, uniform plasma conditions[6]. This project will build upon the knowledge ascertained from previous experiments. Figure 2 shows an example of a buried layer. The material of interest (in our case ^{169}Tm) is sandwiched between a low Z tamp material (plastic or diamond). A short pulse (<2 ps) laser is focused on the tamp layer, generating an energetic, non-thermal bath of hot electrons. The hot electrons have a long mean-free-path, thus depositing a small amount of energy before escaping the target. However, the escaping electrons result in a large return current. The return current heats the buried layer uniformly while the inertial mass of the tamp prevents the layer from expanding. The result is a high temperature, high density plasma confined until the tamp has decompressed into the vacuum. The cooling time can vary depending on the thickness of the tamp, the Z of the buried layer, and the characteristics of the heating laser (laser pre-pulse contrast). For a relatively high contrast pulse ($I_{prepulse}/I \sim 10^{-9}$), the layers will cool relatively fast (< 20 ps)[7].

The atomic emission will be too complicated to use as a density and temperature diagnostic. Thus, an additional thin low Z layer will be placed in contact with the high Z Tm layer. At the expected temperature and density, the low Z layer emission will be simpler H and He like emission, providing a tracer to monitor the plasma density and temperature. Potassium chloride will be used as the tracer layer.

The code FLYCHK[8] was used to estimate the spectral features of the heated Tm and tracer KCl layers (see figure 3). FLYCHK is an atomic population kinetics code used for simulating spectra. The simulations were performed for each layer individually at 1 g/cm^3, 700 eV in non-LTE, steady-state conditions. The K-shell emission from the potassium and chlorine (3.5-4.5 keV) are in a spectral location where the thulium spectra is fairly smooth and would result in minimal added spectral features to the tracer layer emission. However, the L-shell emission from the thulium shows why it is necessary to temporally separate the atomic and nuclear emissions. The predicted atomic L-shell emission lies directly on top of the nuclear transition (8.4 keV).

The experimental plan will be performed in two stages. The first stage will focus on observing the Tm NEEC transition. To separate the atomic and nuclear emission, the LLNL T-REX streak camera will be used[9]. Although the T-REX has demonstrated a temporal resolution of ~600 fs, a much slower setup will be used for the initial experiments to observe the Tm NEEC transition. The spectral resolution for the Tm will be provided by a HOPG crystal spectrometer. This hardware will be built and tested at the LLNL Jupiter Laser Facility during the first year of the project.

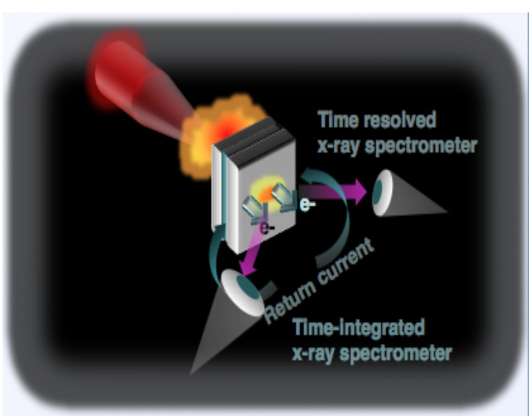

Figure 2: concept of buried layer

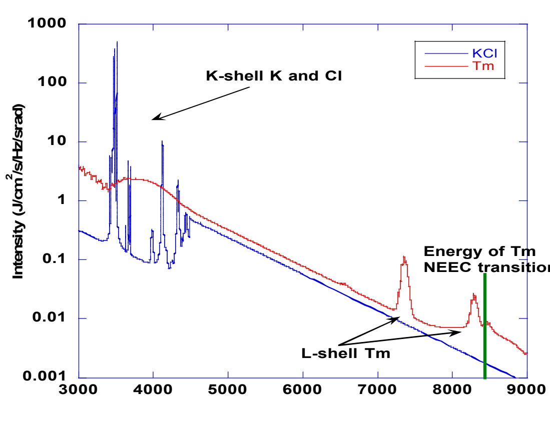

Figure 3: Calculation of K shell tracer and atomic emission from Tm

A second crystal will run simultaneously on the T-REX streak camera to capture the spectra of KCL. This will provide the plasma density and temperature information. Although both crystals will run on the streak camera, only temperature and density data or Tm nuclear transition data will be measured at a given time. This is because of the vastly different time histories of the two emissions. The streak camera will run in fast mode to measure the plasmas conditions or slow mode to measure the time history of the Tm emission.

The experiment will be performed on the Draco laser at Helmholtz-Zentrum Dresden-Rossendorf (HZDR) facility in Dresden Germany. The Draco laser is a 150 TW, Ti:S laser, designed to run at 10 Hz. The LLNL T-REX streak camera was designed as a single-shot diagnostic. As such, the streak camera will be retrofitted to accumulate data at a minimum shot rate of 1 Hz (limited by the streak camera readout).

The second stage of the project will focus on determining the effect the plasma density and temperature have on the nuclear transition half-life. It has been predicted that the transition half-life will decrease as the plasma density and temperature decrease[10] (see figure 4). To test this theory we will try to systematically vary the plasma temperature by adjusting the laser drive energy and change the density by using higher density tamp layer. Simulations show the high Z layer will initial expand into the tamp layer until the pressure of the two materials equalize.

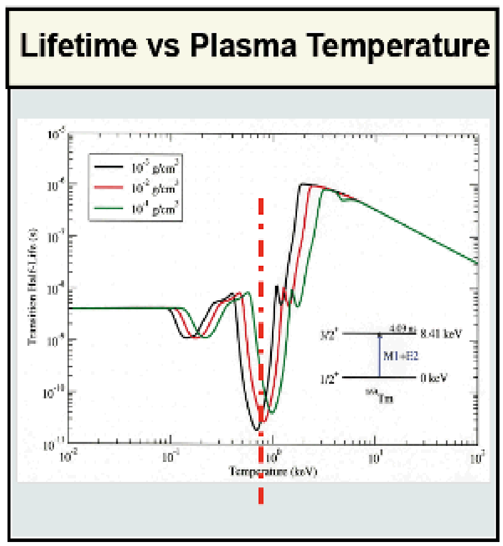

The half-life is predicted to decrease to 30 ps!

Figure 4: Simulation showing the effect of plasma density and temperature on the nuclear transition half-life.

An estimate has been made of the signal size expected from the NEEC transitions. The NEEC process is basically the opposite of internal conversion, i.e., atomic excitation resulting from nuclear decay by the emission of virtual photon. By virtue of detailed balance, in equilibrium the processes are related by a Boltzmann factor. The internal conversion rate is the ratio of the rate of de-excitations by emission of electron to the number of de-excitations by emission of a gamma is given by the factor α. The population of NEEC excited nuclei is represented by N_{NEEC}. A detailed description of the calculation of the NEEC rate is given in reference [11]. For these conditions, α and N_{NEEC} has been estimated as $\sim$ 264 and $\sim 10^{13}$, respectively[12]. Current buried layer experiments performed at the Orion laser facility have shown that it is possible to achieve plasmas at a temperature of >1 keV for about 10 picoseconds at 1g/cm^3. With a layer thickness of 1 μm, the transition rate of $\sim 10^7$/sec is estimated and the number of photons emitted is

$$N_{emitted} \sim (N_{NEEC}) * (transition\ rate) * (\tau_{plasma}) * \left(\frac{1}{\alpha}\right) \sim 4\text{x}10^5\text{, per shot.}$$

When the solid angle and crystal reflectivity are folded in the photons collected per shot is on the order of 10. Hence the images would necessarily get summed together to generate the time-resolved signal. This has been done previously with streak cameras in high rep-rate experiments[13].

Measurement of the electron population relaxation time of a resonantly pumped spectral feature in an Unresolved Transition Array (UTA).

We've begun the design of an experiment to study the accuracy of approximating clusters of atomic transitions with Unresolved Transition Arrays (UTAs). The approximations tend to lead to fairly smooth spectral features when simulating a large number of lines. However, detailed HULLAC simulations show a somewhat large variation in the oscillator strength of the individual lines. So we were wondering if you pumped just a narrow band of lines if the narrow feature would be absorbed with the oscillator strength associated with the narrow band or would it be absorbed with the oscillator strength of the averaged UTA. And once absorbed, how long would it take for the absorbed region to relax back to the shape of the UTA. Potentially this could have a significant effect on calculating opacities of UTAs.

The idea is to look at the accuracy of the approximations used to calculate UTAs. The approximations tend to lead to fairly smooth spectral features when simulating a large number of lines. However, detailed HULLAC simulations show a somewhat large variation in the oscillator strength of the individual lines. So we were wondering if you pumped just a narrow band of lines if the narrow feature would be absorbed with the oscillator strength associated with the narrow band or would it be absorbed with the oscillator strength of the averaged UTA. And once absorbed, how long would it take for the absorbed region to relax back to the shape of the UTA. Potentially this could have a significant effect on calculating opacities of UTAs.

The experiment would use a moderate Z buried layer as a target (say Se). The layer is heated with a short pulse laser (see figure 3).

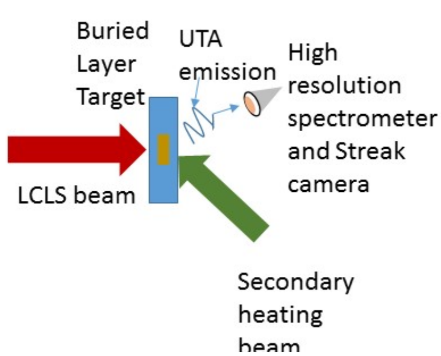

Figure 3: Experimental configuration for LCLS Experiment to study UTA formation

The short pulse laser is focused to generate an (estimated) electron temperature of about 400 eV. The temperature is chosen to create a closed L-shell but an open M-shell. The LCLS beam is used to excite a narrow bandwidth of bound Se electrons from the L-shell into the open M-shell (e.g., - see figure 4a). The time resolved emission from the plasma is measured, centered at the LCLS wavelength in high resolution ( ). The spectral measurement allows us to observe if pumping a narrow portion of the UTA results in excited stated population redistribution into the entire UTA. This (in turn) determines if the assumption of a UTA average oscillator strength, used in simulations, is valid. Ideally, if the emission is spread from the narrow pump energy to the broad UTA, we will measure the time scale for the redistribution.

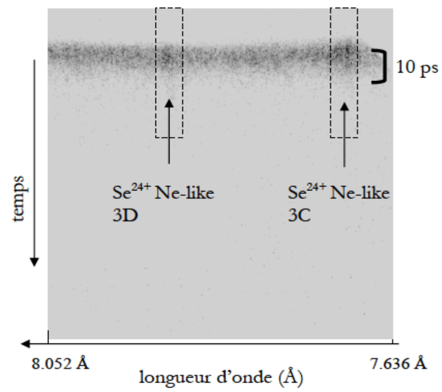

Figure 4a

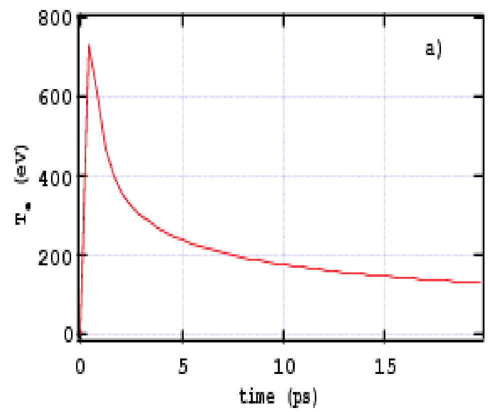

Figure 4b

Also, potentially, the time frame for redistributing the energy to the surrounding bound states (typical time response in figure 1b). The wavelength is scanned across the spectral range of the open M-shell, repeating the initial measurement at different wavelengths of the UTA.

The plasma conditions will be determined using a K-shell tracer layer on top of the Se (maybe Na). We will submit a formal proposal for beam time at the LCLS based on this concept. The proposal will be submitted for beam time next spring (2015).

Preliminary Experiments

To prepare for the laser time awarded in January 2015, two weeks of facility time was provided (in July) to debug the diagnostic suite. Since several diagnostics will be used for the first time at LULI2000, the goal during the two-week period in July was to qualify (or test) the diagnostics and investigate potential problems. Three diagnostics tested: 1) LLNL TREX x-rays streak camera, 2) CEA polycapillary and 5^{th} order polynomial crystal, and 3) LULI/CEA x-ray Fresnel lens.

LLNL TREX Streak Camera

LLNL has provided a TREX sub-picosecond x-ray streak camera for the January campaign. During the two-week diagnostic investigation, the TREX pressure requirements were tested (pump down times), CCD coupling/readout system qualified, and preliminary triggering/timing requirements documented. The TREX requires a chamber pressure of at least 5 x 10^{-5} Torr to operate. The vacuum chamber must be brought to atmospheric pressure to change the target and replace the image plate from other diagnostics. After the target and image plate is replaced, the chamber is evacuated. Existing vacuum capabilities were found to be inadequate so the streak camera was fitted to a secondary chamber that fit inside the facility target chamber. A small opening (~3 mm X 40 mm) was provided for the x-ray to access the streak camera's photocathode and the secondary chamber was differentially pumped. To expedite the pumping, a "cold finger" was added. The completed system resulted in the chamber reaching operating pressure in ~1 hr 20 minutes.

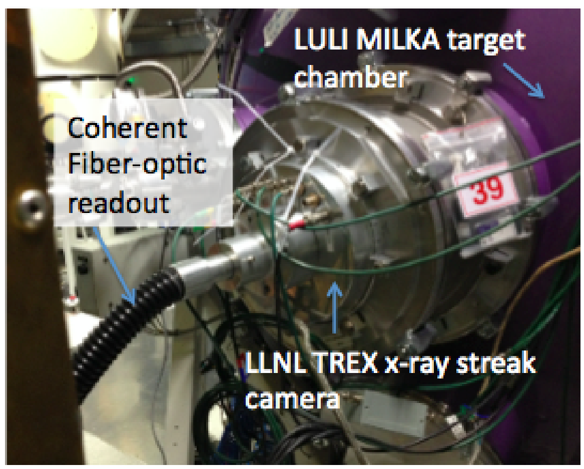

Figure 5: LLNL TREX streak camera mounted on MILKA chamber for testing.

CEA Polycapillaire X/5th order Polynomial Spectrometer

The CEA tested a new x-ray diagnostic design, which allows us to move away the crystal from the target chamber center (TCC). To maximize the x-ray photon collection efficiency, a polycapillary optic is used to collect x-rays from the source. The collected x-rays are diffracted using a (CsAP?) crystal. The crystal is bent in the shape of a 5th order polynomial to maximize collection efficiency while producing spectra along a linear plane. Typically a conical shaped crystal has been used to increase collection efficiency while producing spectra on vertical plane[14]. However, distortions are also a common problem with this method. The 5th order polynomial shape maximizes collection efficiency while minimize image distortions.

To position the detection plane perpendicular to the x-ray beam (for potential use with an x-ray streak camera), and keeping a good spectral resolution, we use a crystal curved along a 5th order polynomial. The 5th order polynomial crystal diffracts x-rays on a linear plane with minimal distortion.

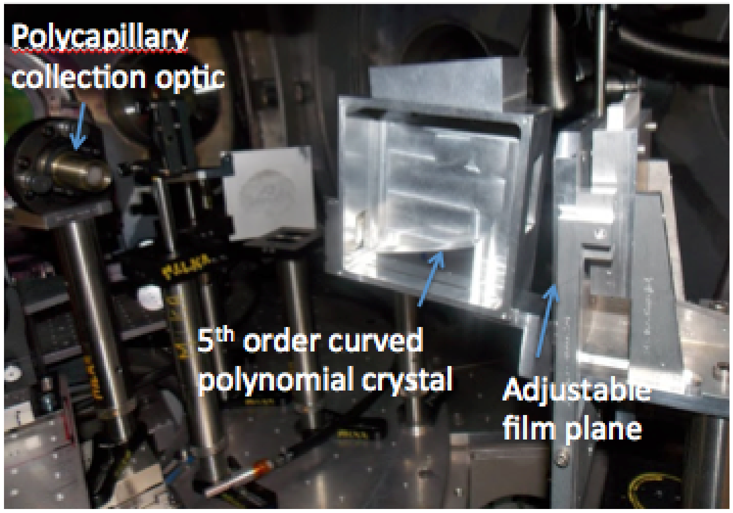

FUHRIX-LULI X-ray Fresnel Lens

Finally, in the planned experiments between the two laboratories it is important to determine the spatial distribution of the X-ray emission (used to determine the plasma characteristics) emitted from the target. This will help benchmark code predictions of the temperature gradients in the sample. Because the source brightness is low and the spatial extent of the source is small (< 50 µm), it is difficult to resolve small features in source. For this measurement, the CEA tested a new x-ray imaging diagnostic utilizing an X-ray Fresnel lens to look at the aluminum He_β ($1s^2$-$1s3p$) transition (used for determining both density and temperature) . The CEA x-ray Fresnel Zone Plate imaging diagnostic (FZP) is capable of a resolution of at least 5 µm spatial resolution at 1880 eV +- 50 eV.

The FZP was used with a multilayered mirror (MM) to provide energy dispersion. The FZP works as a lens in the X-rays domain and has a very high intrinsic resolution while the multilayer mirror provides a spectral resolution of ~ 100 eV. During the summer campaign at LULI2000 the alignment procedure was successfully tested and the resolution was characterized.

Future

The proposed idea of measuring the K_α time history emission from a high Z buried layer was allocated laser time as part of a buried layer campaign that will be performed in January 2015. The LLNL TREX streak camera will be fielded as part of this campaign and will act as a centerpiece for additional collaboration between the two institutions. The LULI is in the process of building a higher power, shorter pulse laser. It is anticipated to begin testing in late 2015-early 2016. Dr. Patrick Audebert and I have begun discussing performing some of the ideas listed here on this facility (along with other possible uses as well).

References

[1] R. Shepherd, et al, “Short pulse laser absorption and energy partition at relativistic laser intensities”, *ERD023-Laboratory Directed Research and Development-Exploratory Research*, Lawrence Livermore National Laboratory (2004).

[2] H. Chen, et al, “Fast-electron-relaxation measurement for laser-solid interaction at relativistic laser intensities”, Phys. Rev. E **76**, 056402 (2007).

[3] Photocathode sensitivity reference

[4] M.R. Harston and J. F. Chemin, “Mechanisms of nuclear excitation in plasmas”, Phys. Rev. C., **59**, no. 5, pg. 2462-2473 (1999).

[5] J. Workman, et al., “Control of Bright Picosecond x-ray Emission from Intense Subpicosecond Laser-Plasma Interactions”, Phys. Rev. Lett., **75**, 12, pg. 2324-2327 (1995).

[6] D. J. Hoarty, et al., “Heating of buried layer targers by 1ω and 2ω pulses using the HELEN CPA laser” High Energy Density Physics, **3**, 1-2, pg. 115-119 (2007).

[7] C. R. Brown, et al., “Measurements of electron transport in foils irradiated with a picosecond time scale laser pulse”, Phys. Rev. Lett., 2011 May 6;106(18).

[8] H.–K. Chung, et al., “FLYCHK: Generalized population kinetics and spectral modeling for rapid spectroscopic analysis for all elements” High Energy Density Physics, **1**, 1, pg. 3-12 (2005).

[9] J. Kuba, et al., “Sub-picosecond streak camera measurements at LLNL: From IR to X-ray”, *Proc. SPIE* 5194, Fourth-Generation X-Ray Sources and Ultrafast X-Ray Detectors, 183 (January 28, 2004); doi:10.1117/12.509702

[10] G. Gosselin, et al., “Modified nuclear level lifetime in hot dense plasma”. Phys. Rev. C **76**, 044611 (2007).

[11] G. Gosselin, et al., “Enhanced nuclear level decay in hot dense plasma”. Phys. Rev. C **70,** 064603 (2004).

[12] A. Kritcher, et al., “Nuclear Excitation by Electron Transition and capture (NEET&NEEC) in laser produced plasmas at Omega (& NIF)”, Joint Institute for Nuclear Astrophysics Workshop-Nuclear Physics in Hot Dense Dynamic Plasmas, March 13th, London, U.K., 2011.

[13] A. Maksimchuk, et al., “Signal averaging x-ray streak camera with picosecond jitter”. Rev. Sci. Instrum., Vol. **67**, No. 3, March 1996.

[14] Conical crystal reference